Agricultural and Forest Meteorology 276–277 (2019) 107615

Contents lists available at ScienceDirect

Agricultural and Forest Meteorology

journal homepage: www.elsevier.com/locate/agrformet

Improving corn yield prediction across the US Corn Belt by replacing air temperature with daily MODIS land surface temperature

Timothy Pede*, Giorgos Mountrakis, Stephen B. Shaw

SUNY College of Environmental Science and Forestry, Department of Environmental Resources Engineering, 402 Baker Lab, 1 Forestry Drive, Syracuse, NY 13210, United States

ARTICLE INFO

Keywords:
MODIS
LST
Corn
Yield
KDD
Prediction

ABSTRACT

While canopy temperature has been extensively utilized for field-level crop health assessment, the application of satellite-based land surface temperature (LST) images for corn yield modeling has been limited. Furthermore, long term yield projections in the context of climate change have primarily employed air temperature (Tair) and precipitation, which may inadequately reflect crop stress. This study assessed potential benefits of satellite-derived LST for predicting annual corn yield across the US Corn Belt from 2010 to 2016. A novel killing degree day metric (LST KDD) was computed with daily LST images from the Moderate Resolution Imaging Spectroradiometer (MODIS) sensor and compared to the typically used Tair-based metric (Tair KDD). Our findings provide strong evidence that LST KDD is capable of predicting annual corn yield with less error than Tair KDD (R^2/RMSE of 0.65/15.3 Bu/Acre vs. 0.56/17.2 Bu/Acre). Even while adjusting for seasonal temperature and precipitation parameters, the R^2 and RMSE of the LST model were approximately 9% higher and 2.0 Bu/Acre lower than the Tair model, respectively. The superior performance of LST can be attributed to its ability to better incorporate evaporative cooling and water stress. We conclude that MODIS LST can improve yield forecasts several months prior to harvest, especially during extremely warm and dry growing seasons. Furthermore, the better performance of LST models over Tair and precipitation models suggest that subsequent long term yield projections should consider additional factors indicative of water stress.

1. Introduction

1.1. Traditional parameters for long term corn yield modeling and crop health assessment

Corn (ie. *Zea mays*) production represents a large portion of both the US and global economy and is vital to the world's food supply. Recent studies have indicated that corn yield may decrease in future years as a result of anthropogenic climate change (Lobell et al., 2011; Butler and Huybers, 2013; Hawkins et al., 2013; Moore and Lobell, 2015). In order to assess food availability in the coming decades, it is crucial to understand climatic effects on corn production.

In an effort to assess future corn supply, a growing body of work has examined the effects of climate and meteorological parameters on corn yield at a regional scale, namely average air temperature (Tair) and total precipitation through the growing season. Corn yield was found to increase with greater seasonal temperatures up to certain threshold (~29–32 °C) and decrease at greater temperatures (Schlenker and Roberts, 2009; Hawkins et al., 2013; Troy et al., 2015), though a strictly negative response was reported in France (Ceglar et al., 2016) and a non-significant, positive response was reported in Pakistan (Ali et al., 2017). Most studies that compared trends in temperature and yield over time (ie. the OLS slope) found an inverse relationship (Lobell and Anser, 2003; Lobell and Field, 2007; Kucharik and Serbin, 2008; Moore and Lobell, 2015). However, a positive relationship has been reported in China (Zhang et al., 2015). A subset of studies focused on yield loss due to heat stress by using the killing degree days concept. Killing degree days (KDD) is derived similar to the more common growing degree day (GDD) metric, but quantifies the extent to which maximum Tair exceeds a threshold for optimal growing conditions (typically 28–30 °C for corn). Multiple authors determined that corn had a positive correlation with GDD and negative correlation with KDD (Butler and Huybers, 2013; Shaw et al., 2014; Butler and Huybers, 2015).

Findings regarding the impact of rainfall are less consistent. On a global scale, trends in growing season precipitation exhibit little to no association with trends in corn yield (Lobell and Anser, 2003; Lobell and Field, 2007). For rainfed counties in the US, a non-linear threshold-type response has been reported (Schlenker and Roberts, 2009; Troy

* Corresponding author.
E-mail address: tjpede@syr.edu (T. Pede).

https://doi.org/10.1016/j.agrformet.2019.107615
Received 13 November 2018; Received in revised form 16 May 2019; Accepted 5 June 2019
Available online 21 June 2019
0168-1923/

et al., 2015), as well a positive response in Wisconsin (Kucharik and Serbin, 2008) and France (Ceglar et al., 2016). Others have found drought frequency or severity, quantified as Standardized Precipitation Index (SPI), to explain a significant portion of variation in corn yield (Zipper et al., 2016; Lu et al., 2017; Mathieu and Aires, 2018). If considered, the relationship between precipitation and corn yield is limited for irrigated counties (Troy et al., 2015; Carter et al., 2016; Zipper et al., 2016), suggesting that the important factor is not necessarily rainfall, but soil moisture.

The extent to which yield loss is derived from heat stress versus water stress is fairly ambiguous, as extreme temperatures can be associated with droughts (Lockart et al., 2009; Hirschi et al., 2011; Mueller and Seneviratne, 2012; Shaw et al., 2014). In addition, Anderson et al. (2015) determined that the sensitivity of corn yield to high temperatures is dependent on water availability. This interaction is confirmed by those who have noted a weaker relationship with growing season temperatures in irrigated districts (Shaw et al., 2014; Troy et al., 2015) and regions experiencing increased precipitation (Schlenker and Roberts, 2009; Leng, 2017a). Rainfall may be an inadequate proxy for soil moisture, especially in areas with deep root zones, such as the US Midwest (Fawcett, 2013; Ransom, 2013). The actual amount of water available to crops (or lack thereof) can depend on a range of factors related to soil and hydrological characteristics, including soil water holding capacity, soil quality and type, rooting depth, water table depth, and land use/land cover (Hund et al., 2009; Hamilton et al., 2015; Licht et al., 2018). Thus, any regional attempt to model corn yield should reflect water availability, as opposed to simply Tair and precipitation.

Canopy temperature is widely accepted as an indicator of field-level crop water stress, since plants close their stomata under water constraints to reduce evapotranspiration and subsequent water loss; this process increases leaf temperatures. When leaf stomata are open, water evaporates and cools the leaf (ie. evaporative cooing) (DeJonge et al., 2015; Han et al., 2016; Mangus et al., 2016; Egea et al., 2017; Carroll et al., 2017). Idso et al (1981) and Jackson (1982) first developed the Crop Water Stress Index (CWSI) to compare canopy temperatures against a non-water stressed (minimum) and water-stressed (maximum) baseline. Numerous follow-up analyses have applied this metric to a variety of crops, often in the context of irrigation scheduling; nearly all measured canopy temperature using a hand-held infrared (IR) thermometer or camera (Taghvaeian et al., 2012; Durigon and de Jong van Lier, 2013; Taghvaeian et al., 2014; DeJonge et al., 2015; Mangus et al., 2016; Carroll et al., 2017).

1.2. Integration of satellite observations in agricultural modeling

Over the past several decades, global land surface temperature (LST) datasets have become available via satellite remote sensing. These earth observation missions include the Moderate Resolution Imaging Spectroradiometer (MODIS), the Advanced Very High Resolution Radiometer (AVHRR), and Advanced Along Track Scanning Radiometer (AATSR) (Alfieri et al., 2013). Due to its superior spatial, spectral, and temporal resolution, MODIS has become the predominant satellite-based sensor for agricultural studies (Ren et al., 2008; Becker-Reshef et al., 2010; Bolton and Friedl, 2013; Zeng et al., 2016; Song et al., 2017).

The majority of analyses that utilize satellite imagery for agriculture modeling do not consider LST and employ Normalized Difference Vegetation Index (NDVI), Enhanced Vegetation Index (EVI), or some other index based on the visible and near-infrared portion of the electromagnetic spectrum (Ren et al., 2008; Becker-Reshef et al., 2010; Sakamoto et al., 2014; Bolton and Friedl, 2013; Shao et al., 2015; Wójtowicz et al., 2016). Other authors have used MODIS Gross Primary Productivity (GPP) to develop a production efficiency model (PEM) or light use efficiency model (LEM) for corn yield prediction (Xin et al., 2013, 2015; Yuan et al., 2016). This approach is based on the assumption that crop yields under non-stressed conditions linearly correlate with the amount of absorbed photosynthetically active radiation. While PEMs have been found to adequately predict annual corn yield in the US Midwest (Xin et al., 2013), they do not incorporate LST, as MODIS GPP is derived from visible, near-infrared, and mid-infrared bands.

The limitation of near-infrared vegetation metrics is that their utility for long term agricultural projection is limited. NDVI primarily reflects the leaf structure and greenness of vegetation (Gamon et al., 1995; Ji and Peters, 2004), which are difficult to predict into the future (Ji and Peters, 2004). Moreover, they do not provide information on the underlying drivers of crop health or growing conditions. LST, however, is more indicative of external controls, such as the surface-energy balance, Tair, and soil moisture. In contrast to NDVI, it is possible to forecast these drivers using a combination of geophysical principals and output from climate change models (Houle et al., 2012; Cuxart et al., 2015; Diallo et al., 2017).

For regional drought assessment, recent studies computed a modified CWSI or similar LST-based water index, such as Temperature Difference Vegetation Index (TDVI), using 8-day and monthly MODIS composites. In this case, the minimum and maximum baselines are alternatively estimated using Normalized Difference Vegetation Index (NDVI) (Khomarudin and Sofan, 2010; Son et al., 2012; Leroux et al., 2016; Bai et al., 2017), Enhanced Vegetation index (EVI) (Holzman et al., 2014; Holzman and Rivas, 2016; Chen et al., 2017; Swain et al., 2017), or Leaf Area Index (LAI) (Dhorde and Patel, 2016). Authors commonly found a strong relationship when these indices were compared to NDVI (Khomarudin and Sofan, 2010), in-situ measurements of soil moisture (Bai et al., 2017), in-situprecipitation (Liang et al., 2014; Bai et al., 2017; Swain et al., 2017), or microwave-based precipitation grids (Son et al., 2012; Chen et al., 2017). Holzman and Rivas (2016) cumulated TDVI over the growing season for an agricultural district of Argentine Pampas, Argentina and found an R^2 of 0.61 with corn yield. LST-based water indices, however, are more suited for heterogeneous landscapes with sparse farmland, which have a range of vegetative conditions to compute the minimum and maximum baselines, and would be less applicable to a homogenous region dominated by agriculture, such as the US Corn Belt. Furthermore, defining the baselines can be an arbitrary, cumbersome process that requires LST/NDVI readings across a variety of vegetative environments (DeJonge et al., 2015; Bai et al., 2017).

Only three studies have related MODIS LST to corn yield in the US. Johnson (2014, 2016) did this on an image-by-image basis using 8-day composites over the course of the growing season. They found that daytime and nighttime LST peaked in August and had relatively low correlations with yield (ρ = -0.58/-0.62 and ρ = -0.29/-0.32, respectively). Heft-Neal et al. (2017) substituted daytime LST for average maximum Tair in an existing climate-response model for corn yield and derived comparable results for the US and improved results for Africa, as a result of sparse weather stations. In all three cases, the authors employed 8-day or monthly composites, which smooth out daily extreme temperatures and do not reflect conditions within critical crop developmental stages.

1.3. Study objectives

There is much evidence to suggest agricultural modeling can be improved by the utilization of daily MODIS LST. However, applications to corn yield have been fairly limited. While authors used LST to estimate Tair and increase the spatial resolution of in-situ GDD (Neteler, 2010; Zhang et al., 2013; Zorer et al., 2013; Alemu and Henebry, 2016), agricultural LST metrics that evaluate the impact of high temperatures (ie. KDD) have yet to be computed directly from LST. Results from this analysis were intended to contribute to two areas of agricultural modeling.

The first is short term, within-season yield prediction (ie. forecasting

yield several months prior to harvest). From an operational perspective, LST could potentially be capable of measuring evaporative cooling across a large region similar to an infrared thermometer at the field-level. Considering canopy temperature's reflection of both heat and water stress, KDD derived from LST may offer significant improvements in regional corn monitoring, yet require relatively simple computations.

The second area is long term, multi-decadal corn yield projection in the context of climate change. Comparing the predictive power of LST and Tair could benefit subsequent climate-yield models, which to date have predominately relied on Tair and precipitation. While LST is not an output of climate models and cannot be directly used for projection, improvements with LST over traditional meteorological factors would suggest that soil and hydrological characteristics indicative of water availability should additionally be considered. A complete understanding of the controls on corn yield requires information regarding both heat and water stress, which are likely better captured by LST.

In this study, we focused on county-level corn yield across the US Corn Belt from 2010 to 2016. The overarching goal was to assess the utility of accumulated degree day metrics derived from satellite-based LST. Our specific objectives were twofold: (i) compare the corn yield predictive capability of KDD derived from Tair and daily MODIS LST and (ii) determine if any improvements remained while controlling for meteorological variables commonly utilized for regional agricultural modeling (ie. GDD, growing season air temperature and precipitation, and drought indices).

2. Methods

2.1. Study area

The US Corn Belt was identified as the study area since it produces nearly three-quarters of the nation's corn (73.3% in 2016 – US Department of Agriculture (USDA, 2018a) and represents a fairly homogeneous, agriculturally dominated landscape (Loveland et al., 1995). The Corn Belt geographic boundaries followed the definition by Green et al. (2018), which is based on a spatiotemporal analysis of land-use patterns and includes 8 states: Illinois (IL), Indiana (IN), Iowa (IA), Minnesota (MN), Nebraska (NE), Ohio (OH), South Dakota (SD), and Wisconsin (WI). Fig. 1 depicts the counties that were utilized for the analysis; refer to Section 2.2 for selection criteria.

As annual NASS Crop Data Layers (CDLs) were only available since 2010 at the time of writing, it was necessary to limit the study period to 7 years from 2010 to 2016. This timeframe encompasses a diverse range of growing conditions, including 2012, which was an unusually warm and dry year, resulting in widespread corn yield loses (Yu et al., 2014; Wang et al., 2016; Lu et al., 2017), as well as 2014 and 2016, which produced higher yields due to preferable temperature and precipitation levels. While long term increases in yield are evident over decades due to continued improvements in breeding and cultivation methods, a span of only 7 years is not extensive enough to reflect an upward trend.

2.2. Data acquisition and preprocessing

This analysis employed MODIS daily daytime 1-km LST (MYD11A1 – version 6) (Wan, 2015); images from the Aqua satellite were selected over Terra because of their ~1:00 PM overpass time for the Corn Belt (vs. 11:00 AM), which is closer to solar noon and consistent with other field-based studies that used canopy temperature to evaluate crop stress (Taghvaeian et al., 2012, 2014; DeJonge et al., 2015; Han et al., 2016; Mangus et al., 2016; Carroll et al., 2017; Egea et al., 2017). MODIS data from 2010 to 2016 for the Corn Belt was downloaded in the Albers Equal Area – WGS 1984 datum/coordinate system courtesy of the USGS Application for Extracting and Exploring Analysis Ready Samples (AppEEARS) (US Geological Survey (USGS, 2018).

Daily 4-km meteorological information was obtained from the Parameter Elevation Regression on Independent Slopes (PRISM) (PRISM Climate Group, 2004). The use of this (Schlenker and Roberts, 2009; Heft-Neal et al., 2017; Lu et al., 2017) or other gridded climate datasets (Lobell and Anser, 2003; Lobell and Field, 2007; Kucharik and Serbin, 2008; Lobell et al., 2011; Hawkins et al., 2013; Troy et al., 2015; Ceglar et al., 2016; Leng, 2017a) is common for regional corn yield modeling. The PRISM variables used for this analysis are daily mean air temperature (Tmean), maximum air temperature (Tmax), minimum air temperature (Tmin), and total precipitation (Precip). Historical monthly precipitation was also used to compute SPI.

County-level annual corn yield (in bushels per acre, Bu/Acre) from 2010 to 2016 was derived from NASS surveys (from Quick Stats 2.0, US Department of Agriculture (USDA, 2018b). The *Counties Cartographic Boundary Shapefile* (1:500,000 scale) defined the boundary and location of counties (US Census Bureau, Geography Division, 2015). Annual NASS Crop Data Layers (CDLs) were also used to isolate majority corn MODIS pixels. Starting in 2010, CDLs provide crop-specific land cover classification at a 30-m resolution for the entire CONUS (US Department of Agriculture (USDA, 2018c). For each year, the

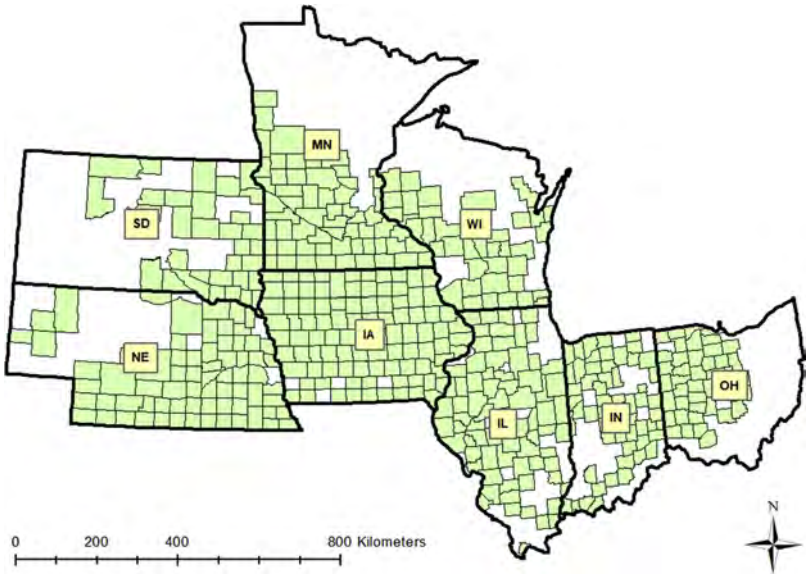

Fig. 1. US Corn Belt states and 463 counties selected for the analysis.

reprojected CDL was used to calculate the percent corn for each 1-km MODIS pixel; those that were > 75% were defined as majority corn. Similar crop masks from CDLs were developed for previous agriculture analyses that employed MODIS images (Bolton and Friedl, 2013; Johnson, 2014, 2016).

Counties were deemed to have sufficient data on the basis of having yield data and at least one majority corn pixel each year during the 7-year study period. This filtering process resulted in a total of 463 counties for the analysis (depicted in Fig. 1). The county boundary layer was reprojected to the datum/coordinate system of the MODIS grids and daily daytime LST values were summarized for each county by taking an average of contained, cloud-free majority corn pixels. To further reduce mixed pixel error, averages were weighted using percent corn, such that pixels with a greater portion of corn land cover were assigned a higher weight. If a county contained no cloud free pixels for a given day, it was assigned a value of "No Data".

The county boundary layer was then reprojected to match the PRISM datum/coordinate system and daily Tmean, Tmax, Tmin, and Precip values were summarized by taking an average of coincident points. PRISM averages were not filtered or weighted by percent corn due the higher spatial resolution of 4-km and fact that pixels are interpolated from in-situ weather stations and do not reflect direct readings. For SPI calculations, monthly PRISM values from 1895 to 2016 were also averaged for counties.

2.3. Computation of killing degree day metrics and univariate analysis

A univariate comparison was initially performed to directly compare LST and Tair corn yield prediction. The traditional killing-degree day metric, subsequently referred to as Tair KDD, was computed from daily Tmax by accumulating values above a specified temperature threshold through the critical developmental period of the corn growing season:

$$Tair\ KDD = \sum_{d=1}^{d=n} KDD_d\ KDD_d$$
$$= \begin{cases} 0\ if\ Tmax < Tair\ Thresh \\ Tmax - Air\ Thresh\ if\ Tmax > Tair\ Thresh \end{cases}$$

Where KDD_d is the KDD computed for a single day, Tmax is the daily maximum temperature, Tair Thresh is the threshold for Tair KDD (29.8 °C), and d = 1 through n corresponds to the start and end of the critical development phase.

Butler and Huybers (2015) determined that corn yield in the US is most affected by extreme temperatures during the early grain filling phase (silking and dough stages). The utilized critical development period for which KDDs were accumulated was defined as July and August, since this approximately corresponds to the start and end of the silking and dough phases for the Corn Belt, respectively (see Table A.1). Different temporal periods for accumulating KDD were tested, but produced similar results. For more details refer to Appendix A.

A novel killing degree day metric, subsequently referred to as LST KDD, was computed through a similar process, only it was necessary to account for "No Data" values resulting from cloud coverage. Rather than accumulating all values above a temperature threshold, KDDs were calculated for cloud-free days by subtracting the temperature threshold from LST (negative differences were set to 0) and taking an average (as opposed to the summation). The average was then multiplied by the number of days in the critical development phase:

$$LST\ KDD = \bar{KDD}_d\ *N\ KDD_d$$
$$= \begin{cases} 0\ if\ LST < LST\ Thresh \\ LST - LST\ Thresh\ if\ LST > LST\ Thresh \end{cases}$$

Where KDD_d is the KDD computed for a single cloud-free day, N is the number of days in the critical development phase, and LST Thresh is the threshold for LST KDD (23.7 °C). This omitted days with invalid data and avoided an unrepresentative number of 0's by assuming cloud-obstructed days had an LST below the threshold. Invalid values were fairly uncommon and on average only represented 23.4% of days through July and August for the selected counties. To assure this assumption did not produce biased results, Tair KDD was alternatively computed using a similar approach (averaging cloud-free daily KDD); nearly identical results were obtained (see Fig. A.5)

Yield predictive capabilities were compared on the basis of the resulting coefficient of determination (R^2) and root mean square error (RMSE) when corn yield was modeled via ordinary least squares (OLS) as a linear function of (i) Tair KDD and (ii) LST KDD. Observations were pooled across counties and years, resulting in 3241 observations (463 counties X 7 years). Heft-Neal et al. (2017), Troy et al. (2015), and Schlenker and Roberts (2009) utilized this data-pooling approach as well. Similar to Butler and Huybers (2013, 2015), yield and KDD were standardized on a county-by-county basis prior to fitting to control for regional effects, such as climate, soils, cultivars, or growing practices. For both variables, a 7-year average was calculated for each county. That average was then subtracted from each county's 7 observations. For example, Adam County, IL's LST KDD for 2010 was 332.1 °C and the 7-year average was 313.6 °C. Thus, the standardized LST KDD in 2010 was 18.5 °C. In this way, greater than average observations had a positive value; less than the average observations had a negative value. Studies that encompassed a longer time frame (ie. 30+ years) standardized variables with a linear trend to reflect increases in yield due to technological improvements and climate change (Lobell et al., 2011; Shaw et al., 2014; Zipper et al., 2016; Zhang et al., 2015; Ceglar et al., 2016; Wang et al., 2016; Leng, 2017a,b; Lu et al., 2017; Mathieu and Aires, 2018). In this case, however, a simple multiyear average was sufficient due to the short 7-year period, for which changes in technology and climate were negligible.

While authors have employed 29 °C as the threshold for Tair KDD (Butler and Huybers, 2013; Shaw et al., 2014; Butler and Huybers, 2015), there is no information available on the ideal LST range for corn. To identify a threshold, LST KDD was iteratively calculated with candidate values from 10 °C to 40 °C in 0.1 °C increments. The optimal threshold was selected as the value that produced the highest R^2 and lowest the RMSE when standardized yield was modeled as a linear function of standardized KDD (via OLS regression). For consistency, this process was repeated to identify a threshold for Tair KDD.

2.4. Comparison of LST and Tair KDD multiple linear regression models

Following univariate comparison, a multiple regresison analysis was performed to determine if improvements in the predictive capability of LST KDD remained while controlling for factors traditionally used for corn yield modeling. The assessed covariates are listed in Table 1.

For simplicity, authors have defined the corn growing season as the summer months of June, July, and August (Lobell and Anser, 2003; Lobell and Field, 2007; Kucharik and Serbin, 2008; Leng, 2017a) or longer period from late Spring to mid Fall to encompass planting and harvesting (Schlenker and Roberts, 2009; Hawkins et al., 2013; Zhang et al., 2015). For the CONUS, annual average state-level planting and harvest dates specified by *NASS Crop Status Reports* have been used as well (Butler and Huybers, 2013; Shaw et al., 2014; Butler and Huybers,

Table 1
List of additional covariates utilized for multiple regression and source.

Variable	Definition	Source
GDD	Growing degree days	PRISM
S_Tmean	Summer mean daily air temperature	PRISM
G_Precip	Growing season total precipitation	PRISM
S_Precip	Summer total precipitation	PRISM
SPI	August 3-month standardized precipitation index	PRISM

2015; Troy et al., 2015). We defined the growing season from May 1st to October 31st, which approximately corresponds to typical planting and harvesting dates for Corn Belt states (see Table A.1).

GDD is usually included in multiple regression models with KDD to explain yield variability in cooler years with few extreme heat events (Butler and Huybers, 2013; Shaw et al., 2014; Butler and Huybers, 2015), but has also been used in the absence of KDD (Anandhi, 2016; Angel et al., 2017). GDD was quantified by accumulating daily mean temperatures within an ideal range over the course of the growing season, similar to Butler and Huybers (2013, 2015). In this case, the upper and lower bounds were defined as 29 and 9 °C, respectively.

Tmean, averaged over the summer (Lobell and Anser, 2003; Lobell and Field, 2007; Kucharik and Serbin, 2008; Leng, 2017a) or entire growing season (Lobell et al., 2011; Hawkins et al., 2013; Moore and Lobell, 2015; Troy et al., 2015; Zhang et al., 2015; Ceglar et al., 2016; Wang et al., 2016; Ali et al., 2017), has been extensively utilized to model corn yield. We only considered average summer mean Tair (S_Tmean), since average growing season mean Tair would have been highly correlated with GDD. For each county, annual S_Tmean was calculated as the average of county mean daily temperatures from PRISM through June, July, and August.

Summer precipitation (Lobell and Anser, 2003; Lobell and Field, 2007; Kucharik and Serbin, 2008; Schlenker and Roberts, 2009) or growing season precipitation (Lobell et al., 2011; Hawkins et al., 2013; Moore and Lobell, 2015; Troy et al., 2015; Zhang et al., 2015; Ceglar et al., 2016; Wang et al., 2016; Ali et al., 2017) is also commonly used to model corn yield. Both were calculated by accumulating daily PRISM precipitation over the corresponding period (June 1st to August 31st for summer; May 1st to October 31st for growing season). Others have used the more mathematically rigorous metric, SPI, which can be interpreted as the number of standard deviations by which observed precipitation deviates from a long term mean (typically 100+ years) (Keyantash and National Center for Atmospheric Research Staff, 2018). Authors found that CONUS corn yield is most sensitive to a short window SPI (1–3 months) during the summer (Lu et al., 2017; Mathieu and Aires, 2018). We, therefore, considered 3-month SPI, since this encompasses June, July, and August, and followed Lu et al. (2017) approach of using monthly historical PRISM data from 1895 to 2016 and fitting a gamma distribution.

Variables were also standardized for the multiple regression analysis on a county-by-county basis as the difference from the 7-year average, with the exception of SPI since it is already standardized. Two linear models for corn yield were fit via an OLS regression: (i) a Tair model, which included Tair KDD and the 5 additional variables and (ii) and a LST model, which included LST KDD and the 5 additional variables. OLS is a common approach for modeling regional corn yield (Lobell and Anser, 2003; Lobell and Field, 2007; Kucharik and Serbin, 2008; Butler and Huybers, 2013; Shaw et al., 2014; Butler and Huybers, 2015; Ali et al., 2017). To assess their relative influence on yield, variables were again standardized by subtracting the mean and dividing by the standard deviation. Variation Inflation Factor (VIF) examination followed to reduce the effects of multicollinearity. Similar to the univariate analysis, multiple regression models were compared on the basis of their adjusted R^2 and RMSE.

3. Results

3.1. Visual correlations

Fig. 2 displays the annual averages of standardized variables for each state. With the exception of MN, corn yield was lowest in 2012 and greatest in 2014, 2015, or 2016, depending on the state. While they varied in magnitude, the series for LST and Tair KDD followed a similar pattern, having the greatest values in 2012 and lowest values after 2013. Precipitation metrics showed a significant decrease in rainfall for 2012.

3.2. Univariate comparison of derived LST and Tair KDD metrics for yield prediction

The R^2 and RMSE between standardized corn yield and Tair KDD peaked at 0.56 and 17.2 Bu/Acre, respectively, with a corresponding temperature threshold of 29.8 °C. LST KDD peaked at a lower threshold (23.7 °C) with a higher R^2 of 0.65 and lower RMSE of 15.3 Bu/Acre (Fig. 3). Thus, LST KDD served as a better predictor of corn yield from 2010 to 2016, as it explained approximately 10% more of the variation and produced estimates with a smaller standard deviation of error (by ~2 Bu/Acre). Note that RMSE values are in standardized yield (ie. difference from the 7-year mean).

Scatter plots between yield and LST/Tair KDD using their respective thresholds are depicted by Fig. 4. Both had a strong linear trend, but LST KDD exhibited less scatter, especially in 2012, the drought year. Even on a year by year basis, LST KDD appeared to better capture the negative relationship with yield.

3.3. Multivariate comparison of derived LST and Tair KDD metrics for yield prediction

3.3.1. Additional air temperature covariates

GDD and S_Tmean also had negative relationships with yield, but captured less yield variability than the KDD metrics (Fig. 5).

3.3.2. Additional precipitation covariates

All 3 of the precipitation metrics exhibited a threshold-type response with corn yield. S_Precip had the greatest R^2 and lowest RMSE when fit with a parabolic function (Fig. 6).

3.3.3. LST and Tair KDD multiple linear regression models

Multiple linear regression was performed to compare the corn yield predictive power of LST and Tair KDD while controlling for commonly utilized meteorological variables. As the three precipitation metrics were highly correlated with VIFs over 10, we eliminated SPI and G_Precip and kept S_Precip since it had the greatest R^2 and lowest RMSE with yield of the three. Although the VIF for S_Tmean was below 10, it had a response similar to GDD and was removed to avoid redundancy. Regression results are listed in Table 2.

Both models had an overall significance for $\alpha = 0.01$, meaning at least one variable was significantly different than 0; all coefficients were significant for $\alpha = 0.01$. The LST KDD model had a higher adjusted R^2 (by ~9%) and lower RMSE (by ~2.0 Bu/Acre). The standardized coefficient for LST and Tair was roughly 4-times larger in magnitude than the coefficients for other covariates, indicating that they, by far, had the greatest influence on yield from 2010 to 2016 across the Corn Belt.

4. Discussion

4.1. Interpretation of results and comparison to previous work

The R^2 and RMSE of Tair and LST KDD remained flat for low thresholds, since these values were less than the maximum temperature for nearly all days. These lower thresholds essentially subtract a constant value from each year's KDD, which does not change the variability in KDD among years. Only at higher thresholds does KDD vary among years. The optimal R^2 and RMSE for Tair KDD occurred near the commonly used threshold of 29 °C (Butler and Huybers, 2013, 2015), which is based on previous field-level analyses that compared yield and growth rates across a range of simulated heat conditions. Our findings indicate that this value is also applicable to regional, county-level data. The highest R^2 for LST was found at 23.7 °C, but there was no peak as there was for Tair KDD. In fact, alternatively using 0 °C for the threshold derived a comparable R^2 of 0.65 and RMSE of 15.4 Bu/Acre. This suggests that there is not an optimal LST level for corn; a higher LST

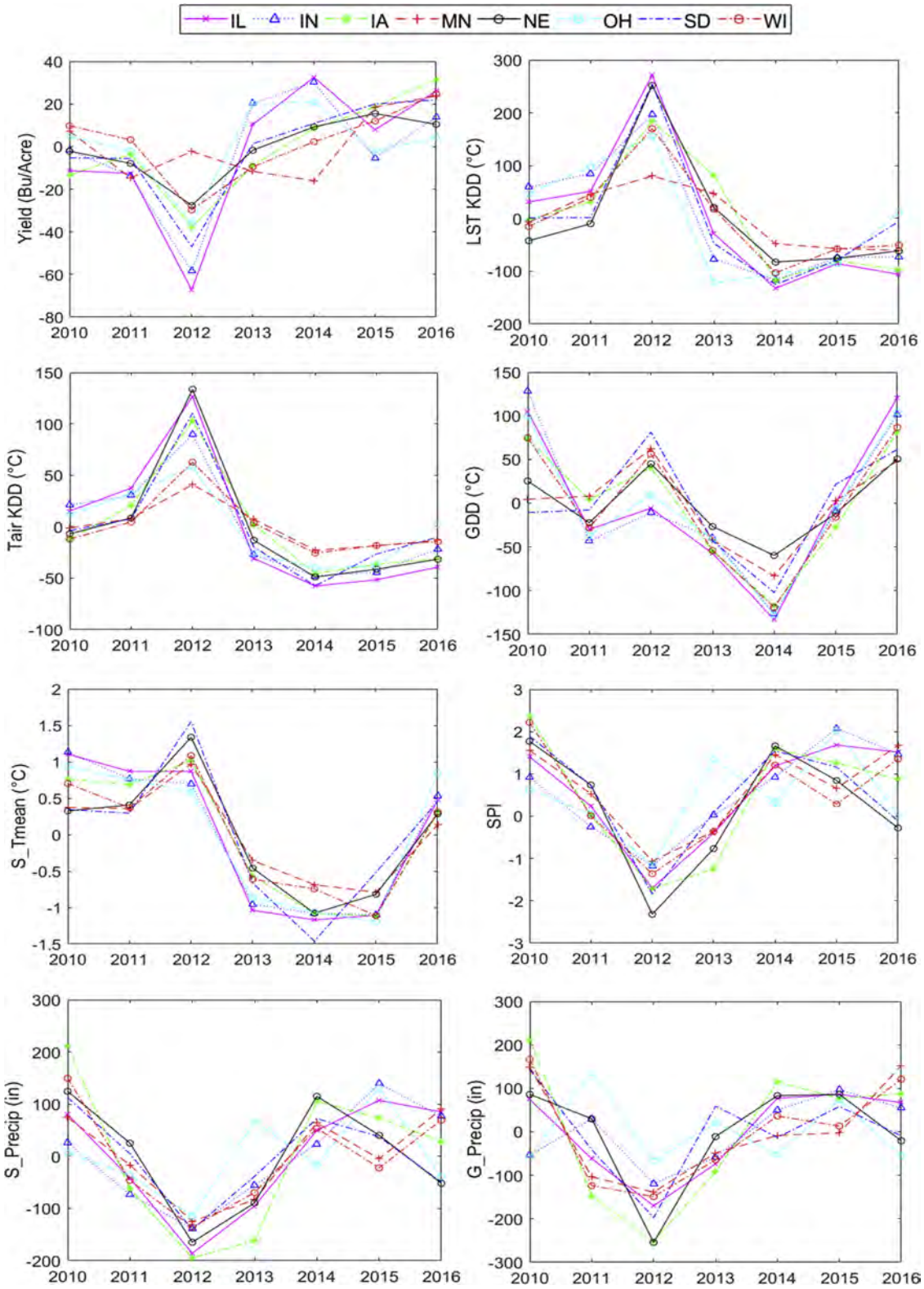

Fig. 2. Time series of standardized corn yield and independent variables, averaged across selected counties for each state by year. Refer to Table 1 for variable definitions.

during July and August across the Corn Belt corresponds to lower yield. This may not, however, be true for other regions with significantly cooler or warmer climates. As the utilized threshold for LST KDD had little effect on results, this metric is essentially a clear sky average of LST multiplied by a constant (the number of days during the critical development period).

The higher R^2 and lower RMSE for both the univariate and multiple linear LST models provide strong evidence that KDD computed from MODIS LST is a superior predictor of corn yield than KDD derived from Tair. In fact, the univariate LST KDD model outperformed the mutliple linear Tair KDD model (R^2/RMSE of 0.65/15.3 Bu/Acre vs. 0.63/15.8 Bu/Acre). Thus, LST alone can provide a better estimate of yield than

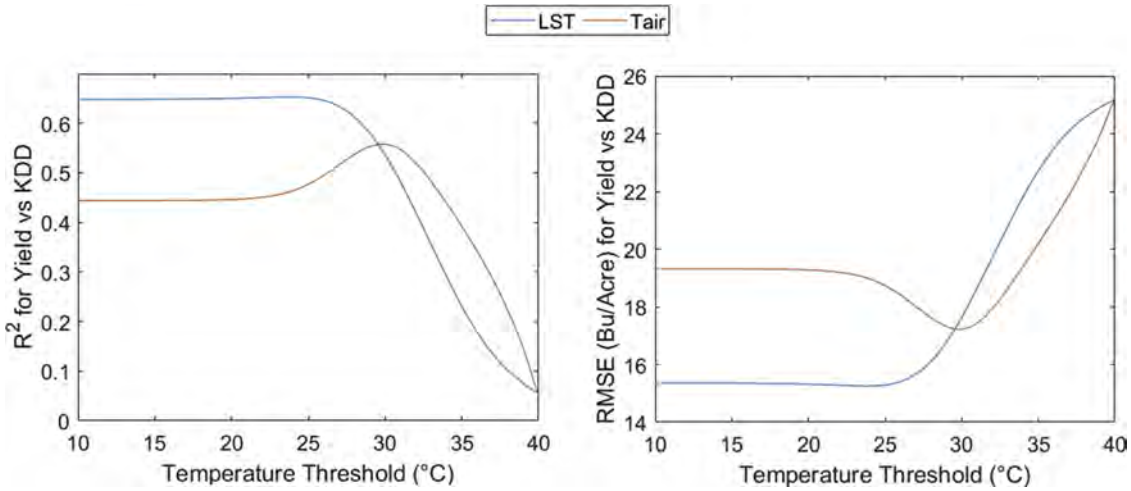

Fig. 3. Coefficient of determination (R^2) (left) and root mean square error (RMSE) (right) for the linear relationship between standardized corn yield and KDD (computed from both LST and Tair) over the range of tested thresholds.

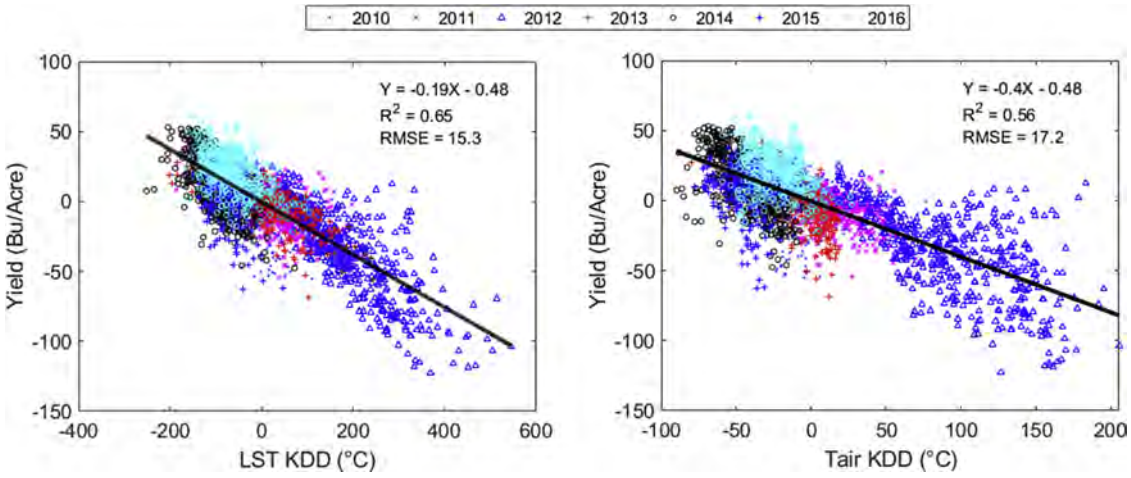

Fig. 4. Scatter plots of standardized LST KDD and Tair KDD vs. yield.

Tair and precipitation combined.

Improvements over Tair were especially apparent in 2012, highlighting LST's ability to reflect water stress. By limiting the univariate regression to observations from 2012, the R^2/RMSE for LST KDD was 0.61/18.8 Bu/Acre, in comparison to Tair KDD's R^2/RMSE of 0.39/23.6 Bu/Acre (Fig. 7). 2012 observations in both scatter plots show considerable separation from other years, but LST KDD does a better job of capturing the linear trend. The two metrics performed worse when 2012 observations were excluded (LST KDD R^2/RMSE = 0.41/14.3 Bu/Acre; Tair KDD R^2/RMSE = 0.28/15.9 Bu/Acre).

Univariate results were similar when fit to state-level data (Fig. B.1). Tair KDD did, however, perform slightly better for WI (R^2/RMSE of

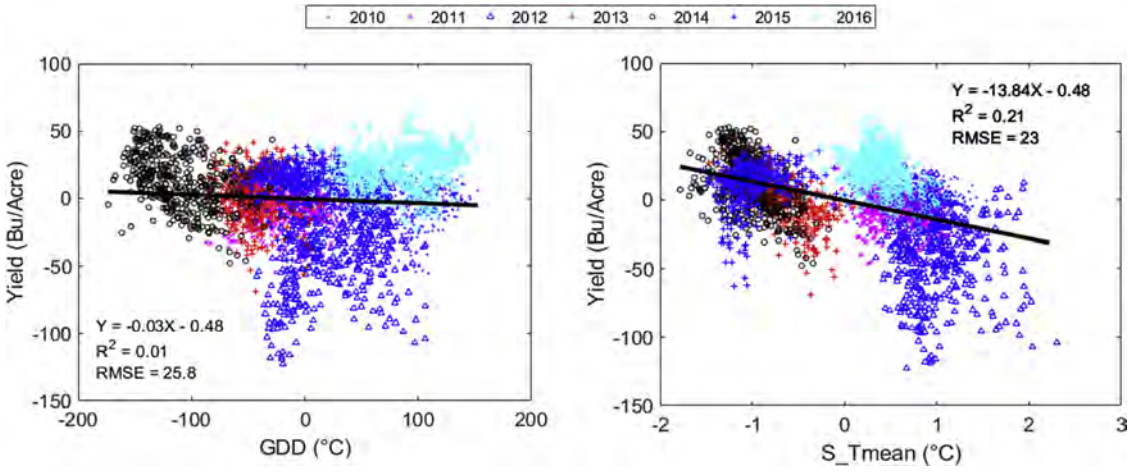

Fig. 5. Scatter plots of standardized GDD and summer mean daily air temperature (S_Tmean) vs. yield.

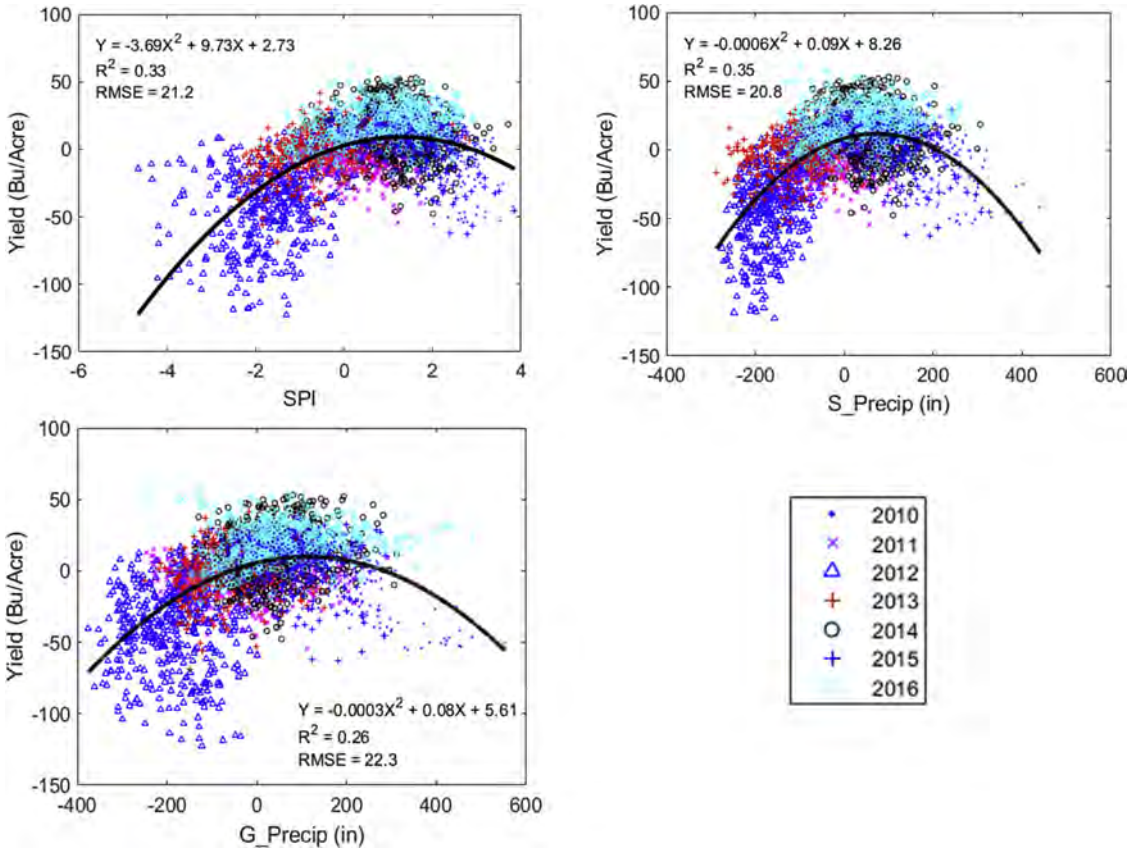

Fig. 6. Scatter plots of standardized precipitation metrics vs. yield; SPI (left), summer precipitation (S_Precip) (right), and growing season precipitation (G_Precip) (bottom).

0.52/15.2 Bu/Acre vs. 0.56/14.5 Bu/Acre). Both LST and Tair KDD poorly predicted corn yield for MN, possibly due to the cooler climate. In comparison to other states, MN experienced fewer extreme temperatures and lower KDDs from 2010 to 2016. As a result, LST/Tair KDD and yield remained relatively stable over the study period. When multiple linear models were fit to just MN data, GDD had a larger standardized coefficient (LST KDD Model: GDD β = 0.60, KDD β = -0.69; Tair KDD Model: GDD β = 0.72 and KDD β = -0.79), indicating yield is more influenced by temperatures within an ideal growing range than extreme heat. Furthermore, the adjusted R^2s of the mutiple linear models were substantially higher than the univariate models (0.59 for LST, 0.50 for Tair). When comparing all states, there was a slight, positive trend between the 7-year mean summer Tair and R^2, suggesting KDD is more predictive of yield in warmer climates (Fig. 8). NE deviates from this trend, possibly due to the higher portion of irrigated crop area, further investigated in Section 4.2.

In agreement with Butler and Huybers (2013), Shaw et al. (2014), and Butler and Huybers (2015), we found a negative correlation with yield for both LST and Tair KDD. Note that our study differs from these as it employed remotely sensed LST to derive KDD, as opposed to Tair.

Surprisingly though, the relationship we found for GDD with yield was slightly negative. This is most likely due to the influence of 2012 data, which contained lower yields but higher GDDs induced by warmer temperatures. A similar relationship with yield occurred for mean summer air temperature (S_Tmean). The coefficient for GDD did become positive in both multiple linear models, which accounted for extreme temperatures with KDD.

Similar to Schlenker and Roberts (2009) and Troy et al. (2015), corn yield exhibited a threshold-type response to precipitation metrics; the relationship was weaker than temperature-based metrics, as reported by Lobell and Field (2007) and Hawkins et al. (2013). In fact, the R^2s were fairly low, supporting the notion that precipitation measured across a network of weather stations inadequately reflects crop water availability. We did not expect summer precipitation to be a better predictor of corn yield than August SPI, especially considering the severity for the 2012 drought. This inconsistency from Mathieu and Aires (2018) could be due to the smaller geographic and temporal extent of our analysis.

Table 2
Multivariate regression results. *Note*: Coefficients are standardized.

LST KDD Model				Tair KDD Model			
Adj. R^2 =	0.72	RMSE =	13.8	Adj. R^2 =	0.63	RMSE =	15.8
Term	*Coeff*	*P-Value*	*VIF*	*Term*	*Coeff*	*P-Value*	*VIF*
Intercept	0.0000	< 0.001	–	Intercept	0.0000	< 0.001	–
LST KDD	−0.9417	< 0.001	2.45	Tair KDD	−0.7854	< 0.001	2.25
GDD	0.1732	< 0.001	1.15	GDD	0.1709	< 0.001	1.18
S_Precip^2	−0.1286	< 0.001	1.28	S_Precip^2	−0.2179	< 0.001	1.19
S_Precip	−0.2067	< 0.001	2.10	S_Precip	−0.0849	< 0.001	1.95

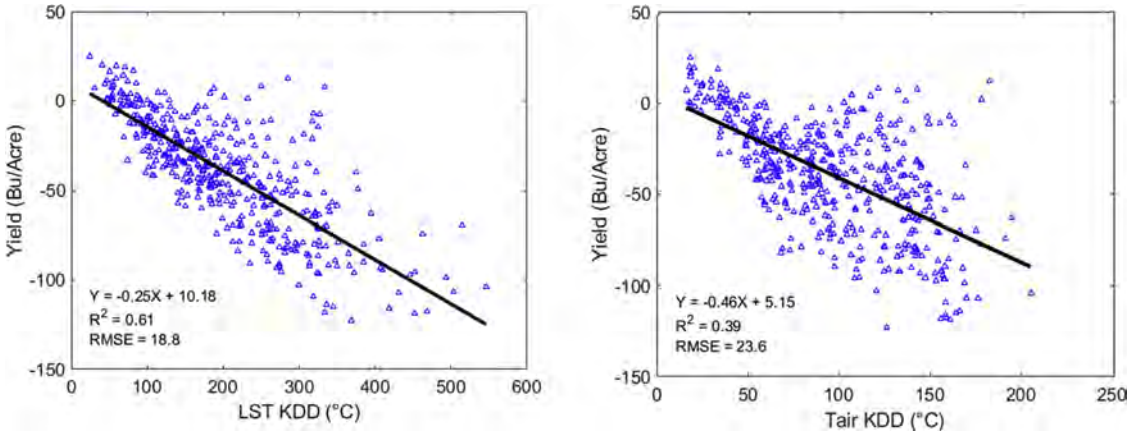

Fig. 7. Scatter plots of standardized LST and Tair KDD vs. yield for 2012 only.

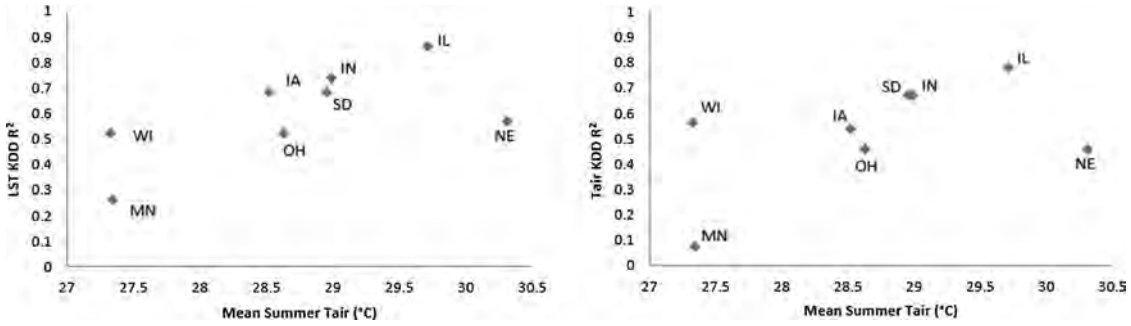

Fig. 8. Univariate model R^2 for LST and Tair KDD for each state vs. mean summer Tair.

Since the multiple linear LST and Tair KDD models exhibited only marginal improvement over univariate models (a ~7% increase in R^2 and ~1.5 Bu/Acre decrease in RMSE), KDD alone can explain the vast majority of inter-annual variation in corn yield from 2010 to 2016. Even while adjusting for commonly utilized meteorological factors, the R^2 and RMSE of the multiple linear LST KDD model remained ~9% higher and ~2.0 Bu/Acre lower than the Tair KDD model. Thus, improvements from the utilization of LST cannot be accounted for by the inclusion of additional meteorological parameters.

The multipl linear LST KDD model compared favorably to previous regional models of corn yield (Table 3). It should be noted that several of these studies incorporated a numerical time variable (ie. year), which to some extent obscures the amount of variation actually explained by climate factors, since the upward yield trend is so strong. As shown by Shaw et al. (2014), including a time parameter can substantially improve the model R^2 (from 0.30/0.44 to 0.71 in the case of Shaw et al., 2014). When our multiple linear LST model is fit on a county-by-county basis, the average R^2 was 0.68 (0.63 for Tair KDD), even without a time variable. While some caution is advised with interpreting direct comparisons, as these analyses utilized different regression approaches, study areas, and explanatory variables, this indicates that our model performed reasonably well, especially when considering the limited temporal extent.

To further compare our findings to previous work (Johnson, 2014, 2016; Heft-Neal et al., 2017), we investigated the extent to which alternatively using 8-day images affected the portion of yield variability explained by LST KDD. This, however, produced similar results to daily images (R^2 = 0.62, RMSE = 15.9 Bu/Acre). Since yield is a single response value summarized for the entire growing season, the loss of daily variation inherent in aggregated 8-day composites does not significantly impact the predictive capability. We also recomputed LST KDD using the entire growing season (May 1st to October 31st). This resulted in a much lower R^2 and higher RMSE of 0.48/18.6 Bu/Acre for LST KDD and 0.50/18.2 Bu/Acre for Tair KDD. It is possible that Heft-Neal et al.'s (2017) finding of LST and Tair comparably predicting yield may have been due to their use of values over a greater extent of the

Table 3
Regression results from previous regional corn yield models. NOTE: FE = Fixed Effect; OLS = Ordinary Least Squares, FGLS = Feasible Generalized Least Squares, Precip = Precipitation, Tmean = mean air temperature, Tmax = maximum air temperature, Tmin = minimum air temperature.

Study	Spatial Extent	Temporal Extent	Method	Covariates	R^2
Heft-Neal et al. (2017)	US, Africa	2003-2014	Fixed Effect	Season LST, Season Precip, Time FE, County FE	0.73
Shaw et al. (2014)	US (100 Counties)	1981-2011	OLS	GDD, KDD, Time	0.30-0.71
Schlenker and Roberts (2009)	US W. of 100 deg	1950-2005	Fixed Effect	Summer Tair, Summer Precip, Time, Counte FE	0.77
Lobell and Field (2007)	Global	1961-2002	OLS	Summer Tmax, Summer Tmin, Summer Precip	0.47
Butler and Huybers (2015)	US	1981-2008	OLS - Bootsrapping	GDD, KDD, Time	0.69
Zipper et al. (2016)	US	1958-2007	OLS	SPI	0.09-0.20
Lobell and Anser (2003)	US	1982-1998	OLS	Simmer Tair, Summer Precip, Summer Solar Radiation	0.25
Kucharik and Serbin (2008)	Wisconsin	1950-2006	OLS	Summer Tair, Summer Precip	0.13-0.40
Ali et al. (2017)	Pakistan	1989-2015	OLS and FGLS	Season Tmax, Season Tmin, Season Precip, Season Humidity, Season Sunshine, Time	0.29

growing season. Moreover, the improved performance of LST mainly pertains to the time phase associated with critical development phase of corn (silking through dough stages).

4.2. Investigating LST's ability to capture water stress and evaporative cooling: A case study comparing rainfed and irrigated counties

One explanation for improved yield estimation with LST is its superior ability to reflect water stress and evaporative cooling. To test this theory, we compared the performance of LST and Tair KDD for irrigated and rainfed counties. Assuming irrigated counties are not subject to water deprivation, examining them separate from rainfed counties would isolate heat stress from water stress. Counties were classified as irrigated if > 70% of the total crop area harvested was irrigated and rainfed if < 30% was irrigated (based on the 2012 US Census of Agriculture). Note that the majority of irrigated counties within the Corn Belt are located in NE (Fig. B.2).

Both KDD metrics produced a lower R^2 and RMSE when fit to irrigated counties (LST KDD R^2 = 0.25, RMSE = 9.8 Bu/Acre; Tair KDD: R^2 = 0.23, RMSE = 9.9 Bu/Acre), consistent with previous findings that corn yield exhibits a weaker relationship with Tair in irrigated areas (Shaw et al., 2014; Troy et al., 2015; Carter et al., 2016). With similar R^2 and RSME values, LST and Tair appear to equally reflect heat stress. When fit to rainfed counties, however, LST KDD outperformed Tair KDD by a wider margin (R^2/RMSE of 0.68/15.2 Bu/Acre vs. 0.60/17.1 Bu/Acre), especially in 2012 (R^2/RMSE of 0.71/16.4 Bu/Acre vs. 0.55/20.3 Bu/Acre). While both metrics similarly measure heat stress, LST is particularly advantageous for capturing water stress, most notably during droughts.

NE makes an interesting case to examine LST's ability to measure evaporative cooling, since there are a comparable number of irrigated (n = 15) and rainfed (n = 25) counties. At the field level, one would expect healthy crops, with sufficient water, to have a lower canopy temperature than Tair. As water becomes limited, evapotranspiration decreases and canopy temperature approaches Tair; in extreme cases, canopy temperature can exceed Tair (Singh and Kanemasu, 1983; Fukuoka et al., 2003; Webber et al., 2017). Authors have noticed significantly lower canopy temperatures for irrigated crops in comparison to nearby rainfed ones (Gardner et al., 1981; Cavero et al., 2009; Vadivambal and Jayas, 2011; Carroll et al., 2017).

For each NE county, the average maximum Tair and daytime LST was taken across cloud-free days through July and August from 2010 to 2016. As irrigated counties were not subjected to water depravation, evapotranspiration levels remained stable and the median LST stayed well below the median Tair, even in 2012. For rainfed counties, however, there was a sharp increase in median LST for 2012, due to decreased evapotranspiration and increased water stress (Fig. 9). Thus, LST is not simply lower than Tair by a constant factor, the difference appears to be dependent on water availability and indicative of yield loss; yields for NE irrigated counties in 2012 (184.9 Bu/Acre) were roughly 2X greater than yields for rainfed counties (96.8 Bu/Acre). Moreover, this demonstrates that MODIS LST can measure regional evaporative cooling across the Corn Belt, similar to an IR thermometer at the field level.

Although it is not possible to compare temperatures of irrigated and rainfed temperatures outside of NE, a similar phenomenon is observed for rainfed counties in other states (see Fig. B.3). There was generally a sharp increase in LST for 2012, causing the difference with maximum Tair to become positive or close to 0; for other years, the difference was negative.

4.3. Exploring an alternative metric: LST – Tair difference

Prior field-level studies focused on irrigation optimization computed CWSI as the difference between maximum canopy temperature and maximum Tair, relative to the vapor pressure deficit. We considered LST and Tair separately since their difference is dependent on humidity and our study area encompassed several states with varying atmospheric moisture levels. In addition, our primary focus was on crop stress measured by KDD. For a follow-up analysis, an analogous county-level metric was calculated by using maximum daily vapor pressure deficit (VPDmax) from PRISM. For each county, valid daily LST readings were subtracted by the corresponding maximum Tair and divided by VPDmax. An average was then taken through July and August.

County-level CWSI exhibited a linear, negative relationship with corn yield from 2010 to 2016, but performed relatively poorly in comparison to LST and Tair KDD (R^2 = 0.41, RMSE = 20.0 Bu/Acre) (Fig. 10). As traditional CWSI uses canopy temperature and Tair both recorded at the same location, values interpolated from a nearby weather station may inadequately reflect the actual temperature conditions of corn fields. At the field level, Tair is traditionally used as a baseline to compare canopy temperature against. A multiyear mean may serve as a better baseline at the regional, county-level.

4.4. Major implications and policy recommendations

An array of short term, early yield forecasting models exist (estimate yield several months prior to harvest), many of which employ NDVI-based vegetation indices (Bolton and Friedl, 2013; Sakamoto et al., 2014; Shao et al., 2015; Wójtowicz et al., 2016).The use of MODIS LST, however, has been limited. The findings in this paper stress the need for future models to incorporate satellite-derived LST, especially values

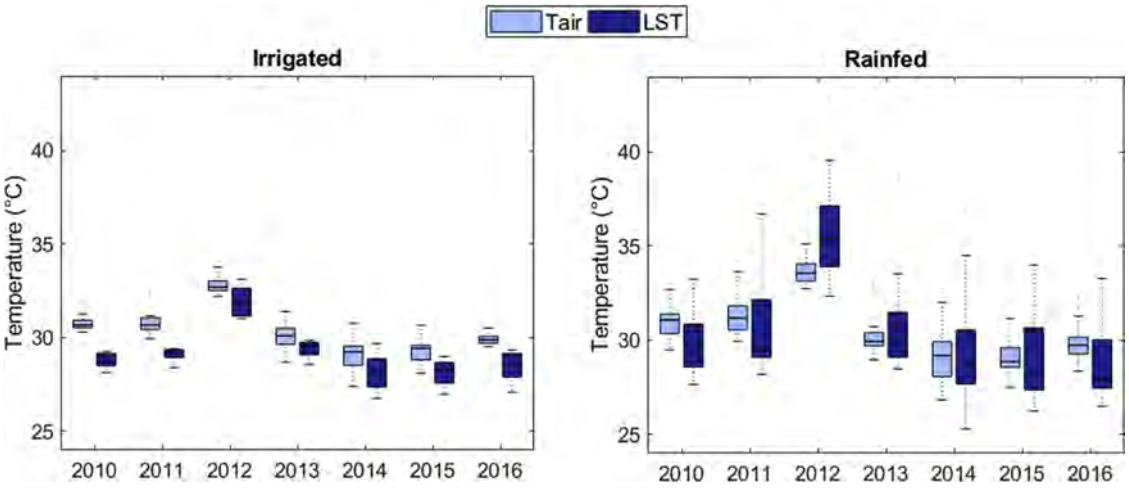

Fig. 9. July-August daytime LST vs. maximum Tair by year for the utilized irrigated and rainfed counties in Nebraska (NE). Created using function by Bikfalvi (2012).

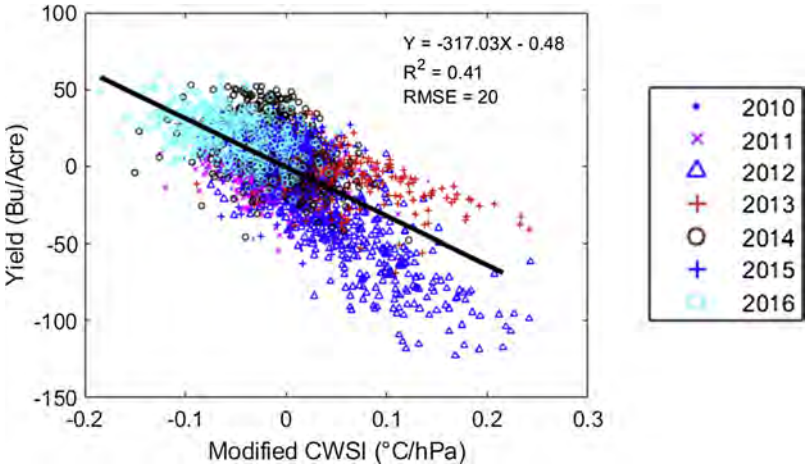

Fig. 10. Standardized county-level CWSI vs. yield.

from the silking and dough development stages. As the LST KDD threshold had little impact on yield prediction and 8-day images produced comparable results, using a simple average of valid composite LST through July and August would suffice.

While corn yield is highly dependent on water availability, in-situ soil moisture measurements at metrological stations are limited and provide a poor spatial coverage (Liang et al., 2014; Escorihuela and Quintana-Seguí, 2016; Bai et al., 2017). This issue is further complicated by the high spatial and temporal variability of soil moisture induced by a range of factors, including topography, rainfall, groundwater level, and soil type (Holzman and Rivas, 2016). In addition, station measurements are typically taken at depths of 5–50 cm, which may not reflect conditions at the actual root depth of corn (Fawcett, 2013; Ransom, 2013; Ford et al., 2015). Obtaining field measurements can be costly, time consuming, and intrusive (Jackson, 1982; Veysi et al., 2017).

MODIS LST can provide an effective means to assess regional water stress across the US Corn Belt, especially in extremely dry years. Considering the frequency and severity of droughts are expected to intensify in the coming decades (Strzepek et al., 2010), this information will become increasingly important for agricultural monitoring. As the USGS Appears platform now allows users to download MODIS products in a custom datum/coordinate system and spatial extent, the USDA or a state agricultural department can easily employ our analytical framework. A similar model could provide within-season forecasts of yield deviation from a 5 to 10 year mean based on average July and August LST. Estimates would be available 1–2 months prior to harvest and 6–7 months before the release of NASS yield reports. Our results indicate that such a model would be more predictive of yield loss due to water stress than existing Tair and precipitation datasets.

Attempts to utilize climate change models for long term future yield projection have relied heavily on predicted changes in Tair and precipitation (Kucharik and Serbin, 2008; Kang et al., 2009; Schlenker and Roberts, 2009; Schlenker and Lobell, 2010; Hawkins et al., 2013; Leng, 2017b). As the improved predictive capability of LST can be attributed to its reflection of evaporative cooling and water stress, the use of Tair and precipitation alone have limitations when employed within statistical models. While LST is not an output from climate models and cannot be directly used for long term corn yield projections, the result from this study suggest that in order to obtain a more complete understanding of the conditions affecting crop growth, prospective models should additionally incorporate variables indicative of water availability. If these are not considered, estimates will contain substantial error in unusually warm and dry growing seasons (such as 2012). Further work is needed to understand how soil moisture at root depth can be modeled as a function of soil conditions and rainfall across different periods of the year. Moreover, MODIS LST can be used as an indicator to help identify potential soil and hydrological characteristics pertinent to yield estimation.

It is important to note that our models were developed via ordinary least squares (OLS) regression. As this method is quite limited, our results only pertain to the US Corn Belt. While more robust regression approaches are available, our intention was not to propose a finalized yield model, but demonstrate the benefits of incorporating LST for yield prediction. Moreover, results pertaining to the Corn Belt have important global food supply implications, as this region produces 73.3% of US Corn and 24.4% of global corn (US Department of Agriculture (USDA, 2018a, 2019).

5. Conclusion

This study investigated the utility of satellite-derived LST for estimating annual corn yield across the US Corn Belt. Our analysis indicates that LST KDD is a better predictor of yield than the common Tair KDD. Even while controlling for metrological variables commonly used for agricultural modeling, the LST KDD model's R^2 and RMSE remained approximately 9% higher and 2.0 Bu/Acre lower, respectively, than the Tair KDD model. In fact, the univariate LST KDD estimates exceeded the multiple linear Tair KDD estimates (R^2/RMSE of 0.65/15.3 Bu/Acre vs. 0.63/15.8 Bu/Acre), suggesting LST alone is a better predictor of corn yield than Tair and precipitation combined. While both metrics equally captured heat stress, improvements with LST are likely due to its ability to reflect water stress and evaporative cooling considering that: (i) LST KDD outperformed Tair KDD by a much wider margin in 2012, a year of severe drought (R^2/RMSE of 0.61/18.8 Bu/Acre vs. 0.39/23.6 Bu/Acre) and (ii) relative year-to-year increases in LST for rainfed counties in Nebraska corresponded more to yield loss than neighboring irrigated counties.

Prior to this analysis, the use of MODIS images for corn yield modeling had primarily involved the near-infrared portion of the electromagnetic spectrum; applications of LST had been limited, especially within the US. The proposed KDD metric is conceptually simple and offers considerable improvements in yield prediction over Tair KDD. While crop health and water availability have traditionally been evaluated at the field-level with an IR thermometer, it was demonstrated that this can be achieved at a regional scale with satellite-based LST. Considering the difficulty of obtaining soil moisture data, MODIS LST would be especially advantageous for within-season early yield forecasts during extremely warm and dry growing seasons.

In the context of climate change, the improved predictive capability of LST indicates that Tair and precipitation alone provide an insufficient representation of water stress. While LST is not an output of climate

models and cannot be directly used to predict future corn yield, subsequent attempts to project yield over several decades should consider a more holistic set of parameters indicative of water availability. If these factors are ignored, estimates may contain substantial error for years with severe drought.

Acknowledgement

This work was supported by a Graduate Assistantship through the Environmental Resources Engineering Department at SUNY College of Environmental Science and Forestry.

Appendix A. and B Supplementary data

Supplementary material related to this article can be found, in the online version, at doi:https://doi.org/10.1016/j.agrformet.2019.107615.

References

Alemu, W., Henebry, G., 2016. Characterizing cropland phenology in major grain production areas of Russia, Ukraine, and Kazakhstan by the synergistic use of passive microwave and visible to near infrared data. Remote Sens. 8 (12), 1016. https://doi.org/10.3390/rs8121016.

Alfieri, S.M., De Lorenzi, F., Menenti, M., 2013. Mapping air temperature using time series analysis of LST: the SINTESI approach. Nonlinear Process. Geophys. 20 (4), 513–527. https://doi.org/10.5194/npg-20-513-2013.

Ali, S., Liu, Y., Ishaq, M., Shah, T., Abdullah, Ilyas, A., Din, I., 2017. Climate change and its impact on the yield of major food crops: evidence from Pakistan. Foods 6 (6), 39. https://doi.org/10.3390/foods6060039.

Anandhi, A., 2016. Growing degree days – ecosystem indicator for changing diurnal temperatures and their impact on corn growth stages in Kansas. Ecol. Indic. 61, 149–158. https://doi.org/10.1016/j.ecolind.2015.08.023.

Anderson, C.J., Babcock, B.A., Peng, Y., Gassman, P.W., Campbell, T.D., 2015. Placing bounds on extreme temperature response of maize. Environ. Res. Lett. 10 (12), 124001. https://doi.org/10.1088/1748-9326/10/12/124001.

Angel, J.R., Widhalm, M., Todey, D., Massey, R., Biehl, L., 2017. The U2U corn growing degree day tool: tracking corn growth across the US Corn Belt. Clim. Risk Manag. 15, 73–81. https://doi.org/10.1016/j.crm.2016.10.002.

Bai, J., Yu, Y., Di, L., 2017. Comparison between TVDI and CWSI for drought monitoring in the Guanzhong Plain, China. J. Integr. Agric. 16 (2), 389–397. https://doi.org/10.1016/S2095-3119(15)61302-8.

Becker-Reshef, I., Vermote, E., Lindeman, M., Justice, C., 2010. A generalized regression-based model for forecasting winter wheat yields in Kansas and Ukraine using MODIS data. Remote Sens. Environ. 114 (6), 1312–1323. https://doi.org/10.1016/j.rse.2010.01.010.

Bikfalvi, A., 2012. Advanced Box Plot for Matlab. Accessed on April 12th, 2018 from:. http://alex.bikfalvi.com/research/advanced_matlab_boxplot/.

Bolton, D.K., Friedl, M.A., 2013. Forecasting crop yield using remotely sensed vegetation indices and crop phenology metrics. Agric. For. Meteorol. 173, 74–84. https://doi.org/10.1016/j.agrformet.2013.01.007.

Butler, E.E., Huybers, P., 2013. Adaptation of US maize to temperature variations. Nat. Clim. Change 3 (1), 68–72. https://doi.org/10.1038/nclimate1585.

Butler, E.E., Huybers, P., 2015. Variations in the sensitivity of US maize yield to extreme temperatures by region and growth phase. Environ. Res. Lett. 10 (3), 034009. https://doi.org/10.1088/1748-9326/10/3/034009.

Carroll, D.A., Hansen, N.C., Hopkins, B.G., DeJonge, K.C., 2017. Leaf temperature of maize and Crop Water Stress Index with variable irrigation and nitrogen supply. Irrig. Sci. 35 (6), 549–560. https://doi.org/10.1007/s00271-017-0558-4.

Carter, E.K., Melkonian, J., Riha, S.J., Shaw, S.B., 2016. Separating heat stress from moisture stress: analyzing yield response to high temperature in irrigated maize. Environ. Res. Lett. 11 (9), 094012. https://doi.org/10.1088/1748-9326/11/9/094012.

Cavero, J., Medina, E.T., Puig, M., Martínez-Cob, A., 2009. Sprinkler irrigation changes maize canopy microclimate and crop water status, transpiration, and temperature. Agron. J. 101 (4), 854. https://doi.org/10.2134/agronj2008.0224x.

Ceglar, A., Toreti, A., Lecerf, R., Van der Velde, M., Dentener, F., 2016. Impact of meteorological drivers on regional inter-annual crop yield variability in France. Agric. For. Meteorol. 216, 58–67. https://doi.org/10.1016/j.agrformet.2015.10.004.

Chen, C.F., Son, N.T., Chen, C.R., Chiang, S.H., Chang, L.Y., Valdez, M., 2017. Drought monitoring in cultivated areas of Central America using multi-temporal MODIS data. Geomat. Nat. Hazards Risk 8 (2), 402–417. https://doi.org/10.1080/19475705.2016.1222313.

Cuxart, J., Conangla, L., Jiménez, M.A., 2015. Evaluation of the surface energy budget equation with experimental data and the ECMWF model in the Ebro Valley. J. Geophys. Res. Atmos. 120 (3), 1008–1022. https://doi.org/10.1002/2014JD022296.

DeJonge, K.C., Taghvaeian, S., Trout, T.J., Comas, L.H., 2015. Comparison of canopy temperature-based water stress indices for maize. Agric. Water Manag. 156, 51–62. https://doi.org/10.1016/j.agwat.2015.03.023.

Dhorde, A.G., Patel, N.R., 2016. Spatio-temporal variation in terminal drought over western India using dryness index derived from long-term MODIS data. Ecol. Inform. 32, 28–38. https://doi.org/10.1016/j.ecoinf.2015.12.007.

Diallo, F.B., Hourdin, F., Rio, C., Traore, A.-K., Mellul, L., Guichard, F., Kergoat, L., 2017. The surface energy budget computed at the grid-scale of a climate model challenged by station data in West Africa: GCM FACING WEST AFRICA IN-SITU DATA. J. Adv. Model. Earth Syst. 9 (7), 2710–2738. https://doi.org/10.1002/2017MS001081.

Durigon, A., de Jong van Lier, Q., 2013. Canopy temperature vs. soil water pressure head for the prediction of crop water stress. Agric. Water Manag. 127, 1–6. https://doi.org/10.1016/j.agwat.2013.05.014.

Egea, G., Padilla-Díaz, C.M., Martinez-Guanter, J., Fernández, J.E., Pérez-Ruiz, M., 2017. Assessing a crop water stress index derived from aerial thermal imaging and infrared thermometry in super-high density olive orchards. Agric. Water Manag. 187, 210–221. https://doi.org/10.1016/j.agwat.2017.03.030.

Escorihuela, M.J., Quintana-Seguí, P., 2016. Comparison of remote sensing and simulated soil moisture datasets in Mediterranean landscapes. Remote Sens. Environ. 180, 99–114. https://doi.org/10.1016/j.rse.2016.02.046.

Fawcett, J., 2013. How deep can roots grow? Crops 36 Accessed on March 2nd, 2018 from. http://magissues.farmprogress.com/wal/WF01Jan13/wal036.pdf.

Ford, T.W., McRoberts, D.B., Quiring, S.M., Hall, R.E., 2015. On the utility of in situ soil moisture observations for flash drought early warning in Oklahoma, USA: SOIL MOISTURE DROUGHT EARLY WARNING. Geophys. Res. Lett. 42 (22), 9790–9798. https://doi.org/10.1002/2015GL066600.

Fukuoka, M., Tani, H., Iwama, K., Hasegawa, T., Jitsuyama, Y., 2003. Difference between canopy temperature and air temperature as a criterion for drought avoidance in crop genotypes under field conditions in Japan. Jpn. J. Crop. Sci. 72 (4), 461–470. https://doi.org/10.1626/jcs.72.461.

Gamon, J.A., Field, C.B., Goulden, M.L., Griffin, K.L., 1995. Relationships between NDVI, canopy temperature, and photosynthesis in three California vegetation types. Ecol. Appl. 5 (1), 28–41.

Gardner, B.R., Blad, B.L., Watts, D.G., 1981. Plant and air temperatures in differentially-irrigated corn. Agric. Meteorol. 25, 207–217. https://doi.org/10.1016/0002-1571(81)90073-X.

Green, T.R., Kipka, H., David, O., McMaster, G.S., 2018. Where is the USA Corn Belt, and how is it changing? Sci. Total Environ. 618, 1613–1618. https://doi.org/10.1016/j.scitotenv.2017.09.325.

Hamilton, S.K., Hussain, M.Z., Bhardwaj, A.K., Basso, B., Robertson, G.P., 2015. Comparative water use by maize, perennial crops, restored prairie, and poplar trees in the US Midwest. Environ. Res. Lett. 10 (6), 064015. https://doi.org/10.1088/1748-9326/10/6/064015.

Han, M., Zhang, H., DeJonge, K.C., Comas, L.H., Trout, T.J., 2016. Estimating maize water stress by standard deviation of canopy temperature in thermal imagery. Agric. Water Manag. 177, 400–409. https://doi.org/10.1016/j.agwat.2016.08.031.

Hawkins, E., Fricker, T.E., Challinor, A.J., Ferro, C.A.T., Ho, C.K., Osborne, T.M., 2013. Increasing influence of heat stress on French maize yields from the 1960s to the 2030s. Glob. Change Biol. 19 (3), 937–947. https://doi.org/10.1111/gcb.12069.

Heft-Neal, S., Lobell, D.B., Burke, M., 2017. Using remotely sensed temperature to estimate climate response functions. Environ. Res. Lett. 12 (1), 014013. https://doi.org/10.1088/1748-9326/aa5463.

Hirschi, M., Seneviratne, S.I., Alexandrov, V., Boberg, F., Boroneant, C., Christensen, O.B., et al., 2011. Observational evidence for soil-moisture impact on hot extremes in southeastern Europe. Nat. Geosci. 4 (1), 17–21. https://doi.org/10.1038/ngeo1032.

Holzman, Mauro E., Rivas, R.E., 2016. Early maize yield forecasting from remotely sensed Temperature/Vegetation index measurements. IEEE J. Sel. Top. Appl. Earth Obs. Remote. Sens. 9 (1), 507–519. https://doi.org/10.1109/JSTARS.2015.2504262.

Holzman, M.E., Rivas, R., Piccolo, M.C., 2014. Estimating soil moisture and the relationship with crop yield using surface temperature and vegetation index. Int. J. Appl. Earth Obs. Geoinf. 28, 181–192. https://doi.org/10.1016/j.jag.2013.12.006.

Houle, D., Bouffard, A., Duchesne, L., Logan, T., Harvey, R., 2012. Projections of future soil temperature and water content for three southern quebec forested sites. J. Clim. 25 (21), 7690–7701. https://doi.org/10.1175/JCLI-D-11-00440.1.

Hund, A., Ruta, N., Liedgens, M., 2009. Rooting depth and water use efficiency of tropical maize inbred lines, differing in drought tolerance. Plant Soil 318 (1–2), 311–325. https://doi.org/10.1007/s11104-008-9843-6.

Idso, S.B., Reginato, R.J., Jackson, R.D., Pinter, P.J., 1981. Foliage and air temperatures: evidence for a dynamic “equivalence point.”. Agric. Meteorol. 24, 223–226. https://doi.org/10.1016/0002-1571(81)90046-7.

Jackson, R.D., 1982. Canopy temperature and crop water stress. Advances in Irrigation, vol. 1. Elsevier, pp. 43–85. https://doi.org/10.1016/B978-0-12-024301-3.50009-5.

Ji, L., Peters, A.J., 2004. Forecasting vegetation greenness with satellite and climate data. IEEE Geosci. Remote. Sens. Lett. 1 (1), 3–6. https://doi.org/10.1109/LGRS.2003.821264.

Johnson, D.M., 2014. An assessment of pre- and within-season remotely sensed variables for forecasting corn and soybean yields in the United States. Remote Sens. Environ. 141, 116–128. https://doi.org/10.1016/j.rse.2013.10.027.

Johnson, D.M., 2016. A comprehensive assessment of the correlations between field crop yields and commonly used MODIS products. Int. J. Appl. Earth Obs. Geoinf. 52, 65–81. https://doi.org/10.1016/j.jag.2016.05.010.

Kang, Y., Khan, S., Ma, X., 2009. Climate change impacts on crop yield, crop water productivity and food security – a review. Prog. Nat. Sci. 19 (12), 1665–1674. https://doi.org/10.1016/j.pnsc.2009.08.001.

Keyantash, J., National Center for Atmospheric Research Staff, 2018. The Climate Data Guide: Standardized Precipitation Index (SPI). Extracted on March 1st, 2018 from. https://climatedataguide.ucar.edu/climate-data/standardized-precipitation-index-spi.

Khomarudin, M.R., Sofan, P., 2010. Crop Water Stress Index (CWSI) estimation using modis data. Int. J. Remote. Sens. Earth Sci. 3. https://doi.org/10.30536/j.ijreses.

2006.v3.a1208.
Kucharik, C.J., Serbin, S.P., 2008. Impacts of recent climate change on Wisconsin corn and soybean yield trends. Environ. Res. Lett. 3 (3), 034003. https://doi.org/10.1088/1748-9326/3/3/034003.
Leng, G., 2017a. Evidence for a weakening strength of temperature-corn yield relation in the United States during 1980–2010. Sci. Total Environ. 605–606, 551–558. https://doi.org/10.1016/j.scitotenv.2017.06.211.
Leng, G., 2017b. Recent changes in county-level corn yield variability in the United States from observations and crop models. Sci. Total Environ. 607–608, 683–690. https://doi.org/10.1016/j.scitotenv.2017.07.017.
Leroux, L., Baron, C., Zoungrana, B., Traore, S.B., Lo Seen, D., Begue, A., 2016. Crop monitoring using vegetation and thermal indices for yield estimates: case study of a rainfed cereal in semi-arid West Africa. IEEE J. Sel. Top. Appl. Earth Obs. Remote. Sens. 9 (1), 347–362. https://doi.org/10.1109/JSTARS.2015.2501343.
Liang, L., Zhao, S., Qin, Z., He, K., Chen, C., Luo, Y., Zhou, X., 2014. Drought change trend using MODIS TVDI and its relationship with climate factors in China from 2001 to 2010. J. Integr. Agric. 13 (7), 1501–1508. https://doi.org/10.1016/S2095-3119(14)60813-3.
Licht, M., Archontoulis, S., Hatfield, 2018. Corn Water Use and Evapotranspiration. Accessed on June 2nd, 2018 from. https://crops.extension.iastate.edu/cropnews/2017/06/corn-water-use-and-evapotranspiration.
Lobell, D.B., Schlenker, W., Costa-Roberts, J., 2011. Climate trends and global crop production since 1980. Science 333 (6042), 616–620. https://doi.org/10.1126/science.1204531.
Lobell, D.B., Field, C.B., 2007. Global scale climate–crop yield relationships and the impacts of recent warming. Environ. Res. Lett. 2 (1), 014002. https://doi.org/10.1088/1748-9326/2/1/014002.
Lobell, D.B., Anser, G.P., 2003. Climate and management contributions to recent trends in US agricultural yields. Science 299 (6509), 1032.
Lockart, N., Kavetski, D., Franks, S.W., 2009. On the recent warming in the Murray-Darling Basin: land surface interactions misunderstood. Geophys. Res. Lett. 36 (24). https://doi.org/10.1029/2009GL040598.
Loveland, T.R., Marchant, J.W., Brown, J.F., Ohlen, D.O., Reed, B.C., Olson, P., Hutchinson, J., 1995. Seasonal land-cover regions in the United States. Pap. Nat. Resour. 475, 339–355.
Lu, J., Carbone, G.J., Gao, P., 2017. Detrending crop yield data for spatial visualization of drought impacts in the United States, 1895–2014. Agric. For. Meteorol. 237–238, 196–208. https://doi.org/10.1016/j.agrformet.2017.02.001.
Mangus, D.L., Sharda, A., Zhang, N., 2016. Development and evaluation of thermal infrared imaging system for high spatial and temporal resolution crop water stress monitoring of corn within a greenhouse. Comput. Electron. Agric. 121, 149–159. https://doi.org/10.1016/j.compag.2015.12.007.
Mathieu, J.A., Aires, F., 2018. Assessment of the agro-climatic indices to improve crop yield forecasting. Agric. For. Meteorol. 253–254, 15–30. https://doi.org/10.1016/j.agrformet.2018.01.031.
Moore, F.C., Lobell, D.B., 2015. The fingerprint of climate trends on European crop yields. Proc. Natl. Acad. Sci. 112 (9), 2670–2675. https://doi.org/10.1073/pnas.1409606112.
Mueller, B., Seneviratne, S.I., 2012. Hot days induced by precipitation deficits at the global scale. Proc. Natl. Acad. Sci. 109 (31), 12398–12403. https://doi.org/10.1073/pnas.1204330109.
Neteler, M., 2010. Estimating daily land surface temperatures in mountainous environments by reconstructed MODIS LST data. Remote Sens. 2 (1), 333–351. https://doi.org/10.3390/rs1020333.
PRISM Climate Group, 2004. Oregon State University. Extracted on January 5th, 2018 from:. http://prism.oregonstate.edu.
Ransom, J., 2013. Crop Water Use and Rooting Depth – Crop Rotation for a Dry Cycle. Accessed on April 10th from. North Dakota State University Extension Agronomist. https://www.ag.ndsu.edu/smallgrains/documents/crop-water-use.
Ren, J., Chen, Z., Zhou, Q., Tang, H., 2008. Regional yield estimation for winter wheat with MODIS-NDVI data in Shandong, China. Int. J. Appl. Earth Obs. Geoinf. 10 (4), 403–413. https://doi.org/10.1016/j.jag.2007.11.003.
Sakamoto, T., Gitelson, A.A., Arkebauer, T.J., 2014. Near real-time prediction of U.S. corn yields based on time-series MODIS data. Remote Sens. Environ. 147, 219–231. https://doi.org/10.1016/j.rse.2014.03.008.
Schlenker, W., Roberts, M.J., 2009. Nonlinear temperature effects indicate severe damages to U.S. crop yields under climate change. Proc. Natl. Acad. Sci. 106 (37), 15594–15598. https://doi.org/10.1073/pnas.0906865106.
Schlenker, W., Lobell, D.B., 2010. Robust negative impacts of climate change on African agriculture. Environ. Res. Lett. 5 (1), 014010. https://doi.org/10.1088/1748-9326/5/1/014010.
Shao, Y., Campbell, J.B., Taff, G.N., Zheng, B., 2015. An analysis of cropland mask choice and ancillary data for annual corn yield forecasting using MODIS data. Int. J. Appl. Earth Obs. Geoinf. 38, 78–87. https://doi.org/10.1016/j.jag.2014.12.017.
Shaw, S.B., Mehta, D., Riha, S.J., 2014. Using simple data experiments to explore the influence of non-temperature controls on maize yields in the mid-West and Great Plains. Clim. Change 122 (4), 747–755. https://doi.org/10.1007/s10584-014-1062-y.
Singh, P., Kanemasu, E.T., 1983. Leaf and canopy temperatures of pearl millet genotypes under irrigated and nonirrigated Conditions1. Agron. J. 75 (3), 497. https://doi.org/10.2134/agronj1983.00021962007500030019x.
Son, N.T., Chen, C.F., Chen, C.R., Chang, L.Y., Minh, V.Q., 2012. Monitoring agricultural drought in the Lower Mekong Basin using MODIS NDVI and land surface temperature data. Int. J. Appl. Earth Obs. Geoinf. 18, 417–427. https://doi.org/10.1016/j.jag.2012.03.014.
Song, X.-P., Potapov, P.V., Krylov, A., King, L., Di Bella, C.M., Hudson, A., et al., 2017. National-scale soybean mapping and area estimation in the United States using medium resolution satellite imagery and field survey. Remote Sens. Environ. 190, 383–395. https://doi.org/10.1016/j.rse.2017.01.008.
Strzepek, K., Yohe, G., Neumann, J., Boehlert, B., 2010. Characterizing changes in drought risk for the United States from climate change. Environ. Res. Lett. 5 (4), 044012. https://doi.org/10.1088/1748-9326/5/4/044012.
Swain, S., Abeysundara, S., Hayhoe, K., Stoner, A.M.K., 2017. Future changes in summer MODIS-based enhanced vegetation index for the South-Central United States. Ecol. Inform. 41, 64–73. https://doi.org/10.1016/j.ecoinf.2017.07.007.
Taghvaeian, S., Chávez, J., Hansen, N., 2012. Infrared thermometry to estimate crop water stress index and water use of irrigated maize in Northeastern Colorado. Remote Sens. 4 (11), 3619–3637. https://doi.org/10.3390/rs4113619.
Taghvaeian, S., Comas, L., DeJonge, K.C., Trout, T.J., 2014. Conventional and simplified canopy temperature indices predict water stress in sunflower. Agric. Water Manag. 144, 69–80. https://doi.org/10.1016/j.agwat.2014.06.003.
Troy, T.J., Kipgen, C., Pal, I., 2015. The impact of climate extremes and irrigation on US crop yields. Environ. Res. Lett. 10 (5), 054013. https://doi.org/10.1088/1748-9326/10/5/054013.
US Census Bureau, Geography Division, 2015. 2015 Counties Boundary File, 1:500,000. Accessed on January 10th, 2018 from:. https://www.census.gov/geo/maps-data/data/cbf/cbf_counties.html.
US Department of Agriculture (USDA), 2018a. National Agriculture Statistics Survey. State-Level Corn Maize Production. Accessed on June 20th, 2018 from:. https://quickstats.nass.usda.gov.
US Department of Agriculture (USDA), 2018b. National Agriculture Statistics Survey. County-Level Corn Maize Yield. Accessed on June 20th, 2018 from:. https://quickstats.nass.usda.gov.
US Department of Agriculture (USDA), 2018c. Crop Scape and Cropland Data Layer - National Download. Accessed on January 10th, 2018 from:. https://www.nass.usda.gov/Research_and_Science/Cropland/Release/index.php.
US Geological Survey (USGS), 2018. Application for Extracting Exploring Analysis Ready Samples (ApPEEARS). Accessed on December 20th, 2017 from. https://lpdaacsvc.cr.usgs.gov/appeears/.
US Department of Agriculture (USDA), 2019. World Corn Production, 2018-2019. Accessed on May 14, 2019 from. http://www.worldofcorn.com/#world-corn-production.
Vadivambal, R., Jayas, D.S., 2011. Applications of thermal imaging in agriculture and food industry—a review. Food Bioproc. Technol. 4 (2), 186–199. https://doi.org/10.1007/s11947-010-0333-5.
Veysi, S., Naseri, A.A., Hamzeh, S., Bartholomeus, H., 2017. A satellite based crop water stress index for irrigation scheduling in sugarcane fields. Agric. Water Manag. 189, 70–86. https://doi.org/10.1016/j.agwat.2017.04.016.
Wan,, Z., 2015. MOD11A2 MODIS/Terra Land Surface Temperature/Emissivity 8-Day L3 Global 1km SIN Grid V006. NASA EOSDIS Land Processes DAAC.
Wang, R., Bowling, L.C., Cherkauer, K.A., 2016. Estimation of the effects of climate variability on crop yield in the Midwest USA. Agric. For. Meteorol. 216, 141–156. https://doi.org/10.1016/j.agrformet.2015.10.001.
Webber, H., Martre, P., Asseng, S., Kimball, B., White, J., Ottman, M., et al., 2017. Canopy temperature for simulation of heat stress in irrigated wheat in a semi-arid environment: a multi-model comparison. Field Crops Res. 202, 21–35. https://doi.org/10.1016/j.fcr.2015.10.009.
Wójtowicz, M., Wójtowicz, A., Piekarczyk, J., 2016. Application of remote sensing methods in agriculture. Commun. Biometry Crop Sci. 11, 31–50.
Xin, Q., Broich, M., Suyker, A.E., Yu, L., Gong, P., 2015. Multi-scale evaluation of light use efficiency in MODIS gross primary productivity for croplands in the Midwestern United States. Agric. For. Meteorol. 201, 111–119. https://doi.org/10.1016/j.agrformet.2014.11.004.
Xin, Q., Gong, P., Yu, C., Yu, L., Broich, M., Suyker, A., Myneni, R., 2013. A production efficiency model-based method for satellite estimates of corn and soybean yields in the Midwestern US. Remote Sens. 5 (11), 5926–5943. https://doi.org/10.3390/rs5115926.
Yu, C., Li, C., Xin, Q., Chen, H., Zhang, J., Zhang, F., et al., 2014. Dynamic assessment of the impact of drought on agricultural yield and scale-dependent return periods over large geographic regions. Environ. Model. Softw. 62, 454–464. https://doi.org/10.1016/j.envsoft.2014.08.004.
Yuan, W., Chen, Y., Xia, J., Dong, W., Magliulo, V., Moors, E., et al., 2016. Estimating crop yield using a satellite-based light use efficiency model. Ecol. Indic. 60, 702–709. https://doi.org/10.1016/j.ecolind.2015.08.013.
Zeng, L., Wardlow, B.D., Wang, R., Shan, J., Tadesse, T., Hayes, M.J., Li, D., 2016. A hybrid approach for detecting corn and soybean phenology with time-series MODIS data. Remote Sens. Environ. 181, 237–250. https://doi.org/10.1016/j.rse.2016.03.039.
Zhang, L., Huang, J., Guo, R., Li, X., Sun, W., Wang, X., 2013. Spatio-temporal reconstruction of air temperature maps and their application to estimate rice growing season heat accumulation using multi-temporal MODIS data. J. Zhejiang Univ. Sci. B 14 (2), 144–161. https://doi.org/10.1631/jzus.B1200169.
Zhang, Q., Zhang, J., Guo, E., Yan, D., Sun, Z., 2015. The impacts of long-term and year-to-year temperature change on corn yield in China. Theor. Appl. Climatol. 119 (1–2), 77–82. https://doi.org/10.1007/s00704-014-1093-3.
Zipper, S.C., Qiu, J., Kucharik, C.J., 2016. Drought effects on US maize and soybean production: spatiotemporal patterns and historical changes. Environ. Res. Lett. 11 (9), 094021. https://doi.org/10.1088/1748-9326/11/9/094021.
Zorer, R., Rocchini, D., Metz, M., Delucchi, L., Zottele, F., Meggio, F., Neteler, M., 2013. Daily MODIS land surface temperature data for the analysis of the heat requirements of grapevine varieties. IEEE Trans. Geosci. Remote. Sens. 51 (4), 2128–2135. https://doi.org/10.1109/TGRS.2012.2226465.